Atmospheric Environment 43 (2009) 4570–4576

Contents lists available at ScienceDirect

Atmospheric Environment

journal homepage: www.elsevier.com/locate/atmosenv

Measuring eddy covariance fluxes of ozone with a slow-response analyser

Georg Wohlfahrt [a,*], Lukas Hörtnagl [a], Albin Hammerle [a], Martin Graus [b], Armin Hansel [b]

[a] Institut für Ökologie, Universität Innsbruck, Sternwartestr. 15, 6020 Innsbruck, Austria
[b] Institut für Ionenphysik und Angewandte Physik, Universität Innsbruck, Technikerstr. 25, 6020 Innsbruck, Austria

ARTICLE INFO

Article history:
Received 31 March 2009
Received in revised form
17 June 2009
Accepted 18 June 2009

Keywords:
Frequency response corrections
Transfer function
Random uncertainty
Flux-gradient method
Cospectra
Grassland

ABSTRACT

Ozone (O_3) fluxes above a temperate mountain grassland were measured by means of the eddy covariance (EC) method using a slow-response O_3 analyser. The resultant flux loss was corrected for by a series of transfer functions which model the various sources of high- and, in particular, low-pass filtering. The resulting correction factors varied on average between 1.7 and 3.5 during night and daytime, respectively. A cospectral analysis confirmed the accuracy of this approach. O_3 fluxes were characterised by a comparatively large random uncertainty, which during daytime typically amounted to 60%. EC O_3 fluxes were compared against O_3 flux measurements made concurrently with the flux-gradient (FG) method. The two methods generally agreed well, except for a period between sunrise and early afternoon, when the FG method was suspected of being affected by the presence of photochemical sources/sinks. O_3 flux magnitudes and deposition velocities determined with the EC method compared nicely with the available literature from grassland studies. We conclude that our understanding of the causes and consequences of various sources of flux loss (associated with any EC system) has sufficiently matured so that also less-than-ideal instrumentation may be used in EC flux applications, albeit at the cost of relatively large empirical corrections.

1. Introduction

The eddy covariance (EC) method (Swinbank, 1951) is thought to represent the most direct approach for quantifying the biosphere-atmosphere exchange of mass and energy (Grünhage et al., 2000; Meyers and Baldocchi, 2005) and has been used for studying the fluxes of a number of air pollutants from/to terrestrial ecosystems (Wesely and Hicks, 2000). In the absence of advection, that is vertical and horizontal fluxes in proportion to the respective mean scalar gradients and wind speeds, the source/sink (S) of some non-reactive scalar χ is given as

$$S = \int_0^h \frac{\overline{\delta\chi}}{\delta t} dz + \overline{w'\chi'}_c(h), \quad (1)$$

where the first term on the right-hand side (RHS) corresponds to the so-called storage flux, i.e. the time-rate-of-change in scalar concentration below the height (h) at which measurements are made (z referring to the vertical direction). The second term on the RHS of Eq. (1) corresponds to the vertical turbulent exchange (the so-called eddy term) given as the covariance between the vertical wind speed (w) and the scalar χ which is corrected (subscript c) for the effects of high- and low-pass filtering as detailed below. The primes denote deviations from the temporal mean calculated by Reynolds decomposition as

$$w' = w - \overline{w}\,,\ \chi' = \chi - \overline{\chi}, \quad (2)$$

with w and χ representing instantaneous values. In case of a reactive scalar, such as ozone (O_3), Eq. (1) still holds, but the both the source/sink and the storage term implicitly include chemical source/sink processes.

The EC method is usually applied with wind speed and scalar concentration measurements being made with a high temporal resolution (5–20 Hz) and with fast response sensors (time response ~ 0.1 s) in order to capture as much as possible of the (small and fast) turbulent fluctuations which carry a significant proportion of the flux (Kaimal and Finnigan, 1994). Any eddy flux contribution not captured due to physical limitations of the flux measurement instrumentation may then be corrected for by multiplying the measured covariance (subscript m) with a so-called frequency response correction factor (β), i.e.

$$\overline{w'\chi'}_c = \beta\,\overline{w'\chi'}_m, \quad (3)$$

* Corresponding author. Tel.: +43 512 5075977; fax: +43 512 5072975.
E-mail address: georg.wohlfahrt@uibk.ac.at (G. Wohlfahrt).

1352-2310/$ – see front matter © 2009 Elsevier Ltd. All rights reserved.
doi:10.1016/j.atmosenv.2009.06.031

with $\beta \geq 1$ (Moore, 1986). There are several ways of deriving frequency response correction factors (for a recent discussion see Massman and Lee, 2002; Shimizu, 2007; Spank and Bernhofer, 2008); common to all approaches is the requirement of an estimate/measurement of what is thought to be the true (unmodified) cospectrum ($S_{w\chi}(f)_{\text{reference}}$; referred to as reference cospectrum in the following), as well as an estimate of the flux loss as a function of frequency (f) or a measured cospectrum ($S_{w\chi}(f)_{\text{measured}}$). Because it is probably the most general method and, as we believe also very instructive, we use the approach put forward by Moore (1986) in the following,

$$\beta = \frac{\int_0^\infty S_{w\chi}(f)_{\text{reference}}}{\int_0^\infty S_{w\chi}(f)_{\text{measured}}} = \frac{\int_0^\infty S_{w\chi}(f)_{\text{reference}}}{\int_0^\infty S_{w\chi}(f)_{\text{reference}} \prod_{i=1}^{n} \varphi_i(f)}, \quad (4)$$

which basically states that the correction factor is equal to the ratio of the reference to the measured cospectrum. The latter is derived by "degrading" the reference cospectrum by a series of transfer functions (φ), which represent n sources of high- and low-pass filtering of the measured covariance. The reference cospectrum is either taken from literature (e.g. Kaimal and Finnigan, 1994) or a site-specific reference cospectrum, usually from high-frequency sensible heat flux measurements, is derived (e.g. Wohlfahrt et al., 2005). Equations for the various transfer functions have been summarised in Moore (1986), Moncrieff et al. (1997), Aubinet et al. (2000), Massman (2000), Shimizu (2007) and Spank and Bernhofer (2008).

Provided that the reference cospectrum and the appropriate transfer functions are known, Eqs. (3) and (4) allow to correct for both high-and low-pass filtering of EC flux measurements. While it is clearly desirable to keep these corrections to a minimum (and thus to measure as much as possible of the true flux), this framework allows to use less-than-ideal instrumentation in EC flux applications (at the trade-off of larger corrections). With the advent of modern sonic anemometry this is not so much relevant for the measurement of the wind components, but rather for the measurement of concentrations of some trace gases – either because no reliable fast response analysers are available for the trace gas of interest or because the application requires low-cost slow-response instrumentation to be used (Horst and Oncley, 1995). In the past slow-response sensors have been used most frequently with a particular method of correcting for the high-frequency loss, termed band-pass eddy covariance method, to estimate latent heat fluxes (Horst and Oncley, 1995; Yasuda et al., 1997; Watanabe et al., 2000; Asanuma et al., 2005). More recently, the disjunct eddy covariance method (Rinne et al., 2001) has gained popularity for measuring fluxes with slow-response sensors (e.g. Turnipseed et al., 2009).

In this paper we report on our attempts to use a slow-response closed-path gas analyser for quantifying O_3 fluxes above a temperate mountain grassland in Austria using the EC method. While fast-response O_3 analysers have been available for some time (Ray et al., 1986; Güsten et al., 1992), these instruments often require substantial maintenance and in some cases continuous cross-calibration against an absolute standard (Coyle et al., 2009; Meszaros et al., 2009). In the following we (*i*) assess the ability of Eq. (4) to capture the flux loss associated with a slow-response ozone sensor by conducting a cospectral analysis, (*ii*) analyse the random uncertainty of the EC O_3 flux measurements, and then (*iii*) compare these measurements against concurrent O_3 flux measurements by means of the flux-gradient (FG) method and literature values.

2. Material and methods

2.1. Study site

The study site is located at a meadow in the vicinity of the village Neustift (47 07′N, 11° 19′E) in the Stubai Valley (Austria) at an elevation of 970 m a s l. in the middle of the flat valley bottom. The fetch is homogenous up to 300 m to the east and 900 m to the west of the instrument tower, the dominant day and nighttime wind directions, respectively. The average annual temperature is 6.5 °C, average annual precipitation amounts to 852 mm. The maximum green area index (area of photosynthetically active plant matter per unit ground area) amounts to around 7.5 m^2 m^{-2}. A detailed description of the study site in terms of soil, vegetation and climate may be found in Hammerle et al. (2008) and Wohlfahrt et al. (2008).

2.2. Eddy covariance

The net ecosystem CO_2, H_2O and O_3 exchange was measured using the eddy covariance method (Baldocchi et al., 1988; Aubinet et al., 2000). The three wind components and the speed of sound were measured by a three-dimensional sonic anemometer (R3IA, Gill Instruments, Lymington, UK), CO_2 and H_2O mole fractions by a closed-path infrared gas analyser (Li-7000, Li-Cor, Lincoln, NE, USA), and O_3 mole fractions by a closed-path UV photometric ozone analyser (49i, Thermo Scientific, Franklin, MA, USA). Air was sucked from the inlet, a distance of 0.1 m from the centre of the sensor volume of the sonic anemometer mounted at 3 m above ground, through a 10 m PTFE tube of 0.004 m inner diameter and through a particle filter (1–2 μm) to a T-piece at a flow rate of 18 l min^{-1}. From there air was diverted through short tubes (0.004 m inner diameter, 0.5 m) to the infrared gas analyser (9 l min^{-1}) and the ozone analyser (1.5 l min^{-1}). The infrared gas analyser, which has a nominal time response of 0.1 s, was operated in the absolute mode, flushing the reference cell with dry N_2 from a gas cylinder at 0.1 l min^{-1}. The ozone analyser was operated with the shortest possible averaging time of 4 s. Raw voltage signals of the CO_2, H_2O and O_3 mole fractions were output to the analogue input of the sonic anemometer, where they were synchronised with the sonic signals, which were acquired at 20 Hz. All raw data were saved to a hard disc of a personal computer for post-processing using the *EdiSol* software (Moncrieff et al., 1997).

Half-hourly mean eddy fluxes were calculated as the covariance between the turbulent departures from the mean of the vertical wind speed and the scalar mole fractions using the post-processing software *EdiRe* (Mauder et al., 2008). Means and turbulent departures there from were calculated by Reynolds (block) averaging. A three-axis co-ordinate rotation was performed aligning the co-ordinate system's vector basis with the mean wind streamlines (Kaimal and Finnigan, 1994). The tube induced time delays of the CO_2 and H_2O signals were determined by optimising the correlation coefficient with the vertical wind velocity (McMillen, 1988) within a given time window. For O_3 this approach turned out to result in noisy and largely variable time lags and therefore the approach devised by Massman (2000) was employed as detailed below. Frequency response corrections were applied to raw eddy fluxes accounting for low-pass (sensor separation, dynamic frequency response, scalar and vector path averaging, frequency response mismatch and the attenuation of concentration fluctuations down the sampling tube) and high-pass filtering following Moore (1986) and Aubinet et al. (2000). Finally, fluxes were corrected for the effect of density fluctuations following Webb et al. (1980). Thereby it was assumed that temperature fluctuations had been sufficiently dampened out in the tube by the time air arrived at the gas

analysers so that only water vapour effects needed to be corrected. As suggested by Ibrom et al. (2007a), H_2O mole fractions, lagged by the same time as CO_2, were used to correct CO_2 fluxes. For O_3, in contrast, no concurrent and collocated H_2O concentrations were available and thus a different approach, based on two extreme scenarios, had to be followed: (*i*) all H_2O fluctuations have been dampened out completely (i.e. no correction) and (*ii*) O_3 fluxes are corrected by the (corrected) latent heat flux measured by the infrared gas analyser, which represent the maximum possible correction. A comparison of O_3 fluxes calculated this way showed that differences between these two extreme scenarios were minimal ($y = 0.99x + 0.03$, $r^2 = 0.99$), and therefore option (*i*) was used in the following. Ideally, water vapour fluctuations should be measured concurrently within the same volume and with the same time response as O_3 or sample air be dried (provided this does not compromise the measurement of the O_3 concentration). The latter approach also has to be followed in case no estimate of the latent heat flux is available.

Half-hourly eddy fluxes were screened for validity by removal of time periods with (*i*) the CO_2, H_2O and O_3 signals outside a specific range, (*ii*) the coefficient of variation for CO_2, H_2O and O_3 concentration and pressure within the gas analysers outside a specific range, (*iii*) the third rotation angle exceeding $\pm 10^\circ$ (McMillen, 1988), (*iv*) the stationarity test for the CO_2, H_2O and O_3 fluxes exceeding 60% (Foken and Wichura, 1996), (*v*) deviation of the integral similarity characteristics larger than 60% (Foken and Wichura, 1996) and (*vi*) the maximum of the footprint function (Hsieh et al., 2000) outside the boundaries of the meadow. Ozone fluxes were also discarded when the measured deposition velocity ($-F_{O_3}/[O_3]$) exceeded the maximum possible, i.e. $1/(R_a + R_b)$, where R_a and R_b are the aerodynamic and quasi-laminar boundary layer resistances (Coyle et al., 2009). Here we report data between 11 July and 20 October 2008 – in total 2267 out of the 4896 half-hourly records met these criteria and were used in the subsequent analysis.

Net scalar fluxes were calculated as the sum of the corrected vertical eddy term and the storage flux, the latter being estimated from the time-rate-of-change of the scalar mixing ratios at the reference height between the current and previous averaging interval. Negative fluxes represent transport from the atmosphere towards the surface, positive ones the reverse.

Flux measurements were accompanied by measurements of the major environmental driving variables using standard meteorological equipment (Hammerle et al., 2008; Wohlfahrt et al., 2008).

2.3. Flux-gradient (FG) method

In the FG method (Meyers et al., 1996; Meyers and Baldocchi, 2005), the flux (F) of some scalar χ, O_3 in the present case, is calculated based on the vertical gradient of χ times an "eddy diffusivity" (k), which is derived from the vertical gradient and flux of a proxy scalar, γ, i.e.

$$F_\chi = -\frac{d\chi}{dz} k_\gamma = -\frac{d\chi}{dz} F_\gamma \frac{dz}{d\gamma}, \quad (5)$$

Here CO_2 and H_2O were used as proxy scalars – the respective fluxes being measured by the EC method (see above), their gradients with another infrared gas analyser (CIRAS-Sc, PP-Systems, Herts, UK). Vertical gradients of O_3 were measured by another UV photometric ozone analyser (APOA 350E, Horiba, Langenfeld, Germany). Intakes of the vertical gradient measurement system, each equipped with a 1–2 μm particle filter, were mounted at 1.5 and 3.5 m, i.e. 2 m apart. Air from the two intakes, switched by four PTFE-coated two-way magnetic valves (TEQCOM, Santa Ana, CA/USA), was analysed alternately in a cycle lasting 180 s. Sample air was drawn through 15 m PTFE tubing at 2 l min^{-1} through the O_3-analyser and then sub-sampled from its outlet at 0.1 l min^{-1} by the infrared gas analyser. During the same time, the other line was continuously flushed at around 10 l min^{-1} by a pump. Allowing 60 s for the analysers to be flushed and concentrations to settle, a data logger (CR1000, Campbell Scientific, Logan, UT/USA) saved the concentrations from each intake, taken every 5 s, as half-hourly averages and managed the switching of the magnetic valves.

During post-processing, mole fractions (CO_2, O_3) and the H_2O partial pressure were converted to mole densities using the ideal gas law. Finally, mole densities from the two intake heights were corrected for density effects following Webb et al. (1980). Thereby we only corrected for the water vapour effect, assuming that air from both heights was analysed at the same temperature, which was warranted for the infrared gas analyser which was kept at a constant temperature of 54.6 °C and was experimentally verified for the O_3 analyser.

Ozone fluxes were excluded from the subsequent analysis when the measured gradients fell below the minimum resolvable gradient (MRG), which was determined as the average ± 1.96 standard deviation during a period of one week when both intakes were mounted at a common height of 2 m above ground. The MRG amounted to 96 μmol m^{-3} (approx. 2.5 ppm), 6 mmol m^{-3} (approx. 0.15 mmol mol^{-1}), and 34 nmol m^{-3} (approx. 0.9 ppb) for CO_2, H_2O and O_3, respectively. Note that the accuracy of the FG method decreases as the reference flux approaches zero.

2.4. Cospectral analysis

Cospectra of the vertical wind speed and CO_2, H_2O and O_3, respectively, were calculated with the *EdiRe* software package: To obtain the high frequency component of the cospectra, each run of 36 000 points was divided into nine segments (4096 points each), the last segment being zero-padded to bring it up to 4096 points. Before employing the Fast Fourier Transform, data were conditioned by removing the mean, linear detrending, and tapering the time series with a Hamming window (Kaimal and Finnigan, 1994). To obtain the low frequency component, the same procedure as above was followed except for data being averaged into 4096 blocks each consisting of nine values. The low and high frequency cospectra were then merged and averaged into 50 logarithmically spaced bins.

3. Results and discussion

3.1. Frequency response corrections

In order to judge how well the transfer function approach (Eq. (4)) is able to account for the flux loss associated with the slow-response ozone analyser, we compare the attenuated reference cospectra against measured cospectra of the vertical wind speed and the O_3 concentration (Fig. 1). The first thing to note in Fig. 1 is that, in contrast to other examples of closed-path EC cospectra which show a weak/medium attenuation in the inertial subrange (e.g. Grelle and Lindroth, 1996; Moncrieff et al., 1997; Ibrom et al., 2007b; Shimizu, 2007; Haslwanter et al., 2009), both the O_3 and CO_2 cospectra fall off much more sharply to and below zero at 0.06 and 0.4 normalised frequency, respectively. This feature is due to the fact that these data have not been corrected for any phase shift. Due to the slower time response, cospectra of O_3 start to fall off at lower frequencies as compared to CO_2, which peaks at about the same frequency as the sensible heat cospectrum. The latter is in good accordance with the normalised peak frequency (ca. 0.07) suggested by the model of Kaimal and Finnigan (1994) for unstable

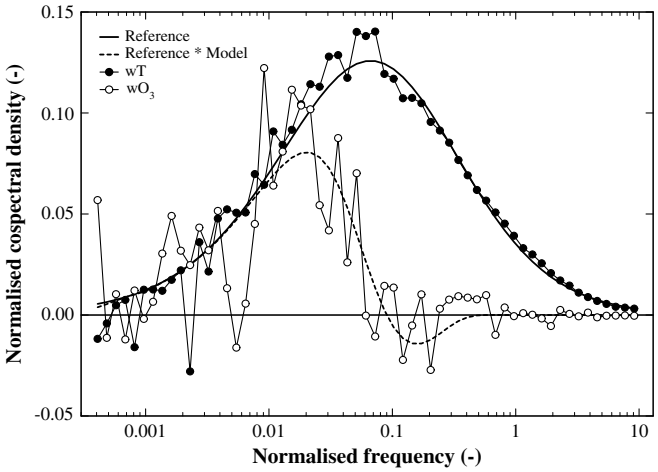

Fig. 1. Comparison between cospectra of sensible heat, O_3 and CO_2 fluxes (symbols) against our cospectral reference model (solid line; Wohlfahrt et al., 2005) and the reference model attenuated by a series of transfer functions (dotted lines), separately for the setup of the O_3 and CO_2 EC flux system. Data refer to unstable conditions and have been averaged over a period of one month. Note that measured O_3 and CO_2 time series have not been corrected for any phase shift.

conditions. The narrow range between ca. 0.001–0.01 normalised frequency, where the three cospectra overlap, corresponds to the so-called band-pass frequency range of the homonymous variant of EC method (Horst and Oncley, 1995; Yasuda et al., 1997; Watanabe et al., 2000; Asanuma et al., 2005). In the band-pass EC method, which in the past has been used frequently for dealing with slow-response scalar sensors, this frequency range is used for scaling the scalar flux of interest to a reference (usually the sensible heat) flux measured with a fast-response sensor. In calculating the overall transfer functions for O_3 and CO_2 (shown as dotted lines in Fig. 1), we have accounted for the following effects: block averaging (Massman, 2000), dynamic frequency response (Moore, 1986), frequency response mismatch (Moore, 1986), scalar and vector path averaging (Moore, 1986), attenuation of concentration fluctuations down the sampling tube (Massman, 1991) and total phase shift (Massman, 2000). These transfer functions are widely used and have been summarised in several papers (e.g. recently by Shimizu, 2007; Spank and Bernhofer, 2008), except probably for the total phase shift (Massman, 2000):

$$\varphi_{\text{phase}}(\omega) = \cos\left[\omega\left(\frac{l_{\text{lon}}}{u}+\frac{L_t}{U_t}\right)\right] - \omega\tau_\beta \sin\left[\omega\left(\frac{l_{\text{lon}}}{u}+\frac{L_t}{U_t}\right)\right]. \quad (6)$$

Here l_{lon} and L_t refer to the longitudinal sensor separation (which is a function of wind direction) and the tube length (m), respectively and u and U_t to the horizontal wind speed and tube flow velocity (m s^{-1}), respectively. τ_β refers to the intrinsic time constant of the scalar sensor (s) and $\omega = 2\pi f$. It is Eq. (6) which is responsible for negative values of the overall transfer function, as all other component transfer functions are bound between 0 and 1 (Massman, 2000). The major difference to the commonly used maximum cross-correlation method (e.g. McMillen, 1988) for accounting for any phase shift between the vertical wind speed and scalar time series is that with this method corrections are done in frequency rather than time space. The latter is often ill-advised when fluxes are low and moreover allows only discrete time shifts (e.g. 50 ms with a 20 Hz sampling frequency). As shown in Fig. 1, the overall transfer function is very well able to mimic the observed attenuation of the O_3 and CO_2 cospectra – the differences in shape being solely due to the different time responses of the scalar instruments, as all other parameters are the same. To our knowledge this represents the first application of Massman's (2000) phase shift transfer function to real-world closed-path EC flux measurements.

The physical setup of a closed-path EC system (including tube flow velocity) assumed constant, frequency response correction factors depend only on atmospheric stability, which affects the shape of the reference cospectrum, wind speed, which affects the distribution of cospectral density across the frequency range, sonic path averaging and longitudinal and lateral sensor separation, and wind direction, which affects the longitudinal and lateral sensor separation (Massman, 2000). Fig. 2 shows the mean diurnal course of the O_3 frequency response correction factors, as well as their wind speed and stability dependency. Frequency response correction factors are generally lower during nighttime hours (1.7–2.0), when wind speeds are low, and increase on average up to 3.5 during early afternoon conditions. During nighttime, lower wind speeds, which cause the cospectrum to shift towards lower frequencies (frequency normalised by $(z_{\text{ref}} - d)/u$, where z_{ref} and d refer to the measurement and zero-plane displacement height, respectively), offset the influence of stable atmospheric conditions, which shift the cospectrum to higher frequencies (Kaimal and Finnigan, 1994). This offset is particularly pronounced at our site, which is characterised by very calm nights and a relatively modest, as compared to the cospectra described in Kaimal and Finnigan (1994), shift towards higher frequencies during stable conditions (Wohlfahrt et al., 2005). Fig. 2 gives an impression of the 'costs' in terms of empirical corrections associated with using the slow-response O_3 analyser, which are appreciable, in particular during daytime conditions when O_3 deposition may be expected to be highest (Coyle et al., 2009; Meszaros et al., 2009). For comparison, frequency response correction factors for closed-path EC systems with fast-response scalar instruments typically range between 1.05 and 2.0 (Grelle, 1997; Moncrieff et al., 1997; Spank and Bernhofer, 2008; Haslwanter et al., 2009), although correction factors up to 5 have been reported by Ibrom et al. (2007b) for water vapour fluxes during conditions of high relative humidity. Note however that these studies accounted for the tube time lag by maximising the cross correlation (McMillen, 1988) and not by employing the phase shift transfer function (Massman, 2000) and thus implicitly yield lower correction factors.

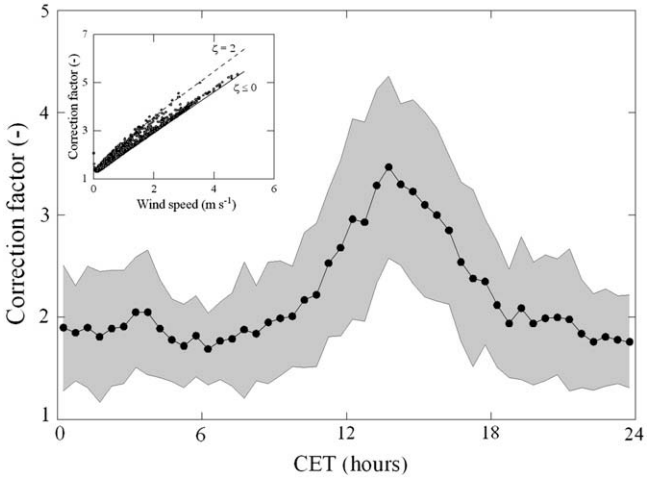

Fig. 2. Mean diurnal course (main panel) and wind speed dependency (inset) of the O_3 flux frequency response correction factors (Eq. (4)). Grey areas in the main panel refer to ±1 standard deviation, lines in the inset to frequency response correction factors simulated for unstable ($\zeta \leq 0$) and stable ($\zeta = 2$) conditions, where ζ refers to the Monin–Obukhov stability parameter. CET refers to central European time.

3.2. Random uncertainty

Another issue with the slow-response O_3 flux measurements is their random (run-to-run) variability, which is already evident in the, as compared to sensible heat and CO_2, much noisier average cospectra (Fig. 1). For a more formal analysis of the random uncertainty we have adopted the successive-day approach devised by Hollinger and Richardson (2005) and Richardson and Hollinger (2005), the results of which are shown in Fig. 3. Briefly, with this approach random uncertainties are derived from pairs of measurements under (close to) identical environmental conditions on successive days, the difference being a reasonable approximation of the random flux uncertainty (Hollinger and Richardson, 2005). In comparison to the CO_2 fluxes measured with the fast-response infrared gas analyser, O_3 fluxes exhibit a higher proportion of measurements with intermediate to large random uncertainties, resulting in a less narrow-peaked frequency distribution (Fig. 3). The same holds for the relative flux uncertainty, i.e. the random uncertainty divided by the flux, which is also clearly higher for the O_3 as opposed to the CO_2 flux measurements (Fig. 3). During typical daytime conditions, the fractional O_3 flux error amounts to around 60%, which is almost twice as high as the random error reported by Finkelstein and Sims (2001) for O_3 flux measurements with a fast-response chemoluminescence O_3 analyser (Ray et al., 1986). Most likely, this is due to an increase in noise of the slow-response O_3 analyser associated with the need to choose the shortest possible integration time (4 s) available. Along this line, we also observed upward-directed O_3 fluxes during approximately 20% of all times (Figs. 3 and 4), which is considerably higher than the 1% fraction

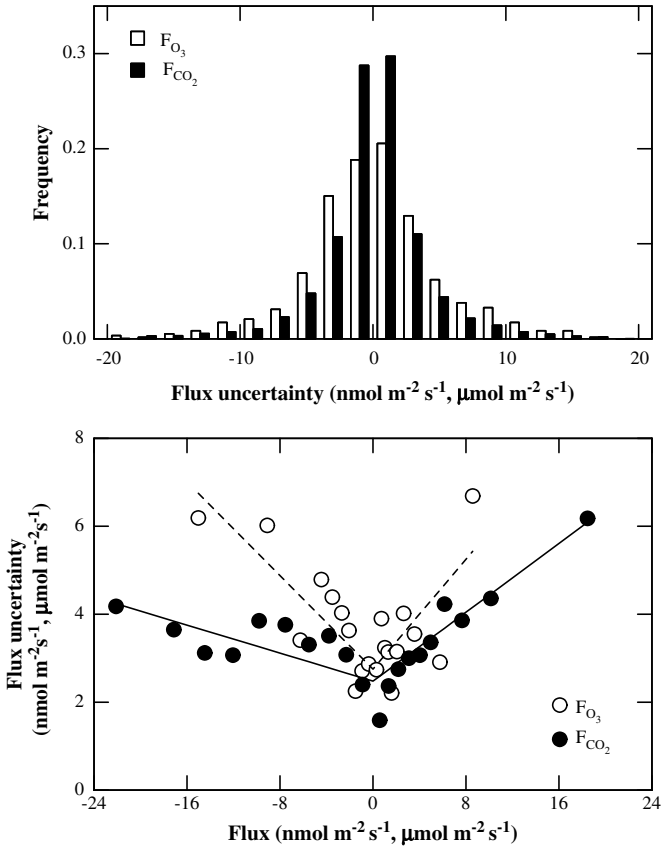

Fig. 3. Random uncertainty of O_3 and CO_2 flux measurements derived according to Hollinger and Richardson (2005) and Richardson and Hollinger (2005). The upper panel shows the frequency distribution of the random flux uncertainty and the lower panel the random flux uncertainty as a function of the flux magnitude.

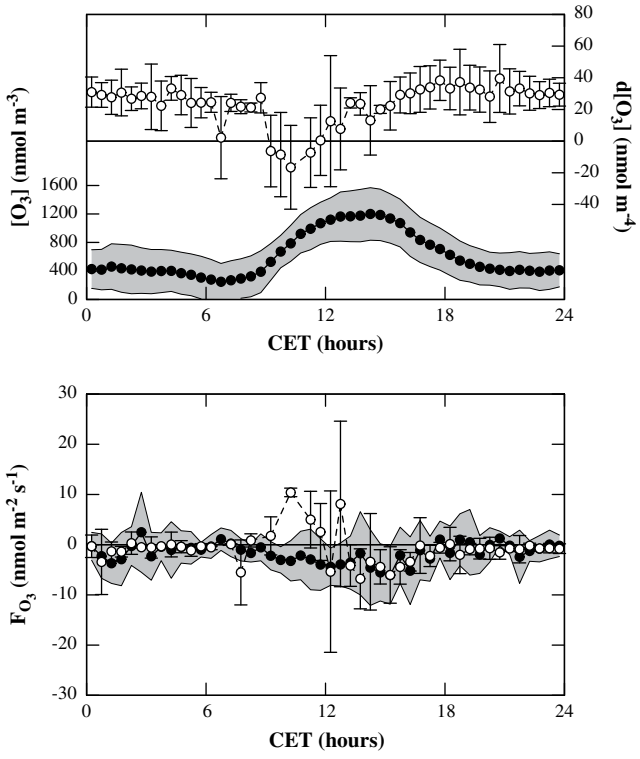

Fig. 4. Mean diurnal courses of O_3 molar density (at 3.5 m height; closed symbols) and vertical O_3 molar density gradients (open symbols) of the flux-gradient (FG) system (upper panel). Comparison of mean diurnal courses of FG (open symbols) and EC (closed symbols) O_3 fluxes (lower panel). Error bars and shaded areas refer to ±1 standard deviation.

reported by Sun and Massman (1999) or the occasional upward transport observed during the growing period by Zeller and Hehn (1996). It therefore seems advisable to average our O_3 flux data over some longer time intervals for obtaining statistically meaningful results (e.g. as in Fig. 4), as errors in means and variances diminish with increasing size of the data set (N) according to $N^{-0.5}$ (Moncrieff et al., 1996).

3.3. Comparison of EC ozone flux determination with FG method and literature

The mean diurnal EC O_3 fluxes compared generally well with FG measurements, except for the period between sunrise (06:30 CET) and ca. 14:30 CET (Fig. 4). This period coincided with the onset of photochemical O_3 production in the morning, indicated by a rise in ambient O_3 mole fractions, and the diurnal O_3 maximum (Fig. 4). During this time vertical O_3 molar density gradients declined from relatively constant nighttime values of approximately 30 nmol m^{-4} towards negative values and then back to nighttime values (Fig. 4). Note that during this cross-over, a large fraction of the measured O_3 gradients was below the MRG and thus excluded from the analysis. We interpret this peculiar behaviour, an upward flux of O_3 during times with maximum evaporation and surface conductances (Hammerle et al., 2008), as an indication of the violation of one of the fundamental assumptions of the FG, i.e. that no sources or sinks of O_3 exist between the upper and lower intake level (Meyers et al., 1996; Grünhage et al., 2000; Meyers and Baldocchi, 2005). We hypothesise that the true (positive) O_3 gradient during this time was masked either by photochemical production of O_3 from NO_2 at the lower intake height, possibly fuelled by the volatile organic compounds emitted by the grassland canopy (Davison et al., 2008),

Table 1
Literature review of average maximum daytime ozone fluxes ($F_{max}O_3$) and deposition velocities (V_{d_max}) measured over grasslands.

Reference	$F_{max}O_3$ (nmol m^{-2} s^{-1})	V_{d_max} (mm s^{-1})	Method
Bassin et al. (2004)	−5.5		EC
Cieslik (1998)		3	EC
Cieslik (2004)	−8		EC
Fowler et al. (2001)		6	AD/EC
Horvath et al. (1998)		1.9	AD
Massman et al. (1995)	−8.3		EC
Meszaros et al. (2009)	−8.3	6	EC
Meyers et al. (1998)		4	EC
Sorimachi et al. (2003)	−4	4	AD
This study	−8	4	EC

EC, eddy covariance method; AD, aerodynamic method.

or by NO_x titration at the upper intake level (Sillman, 1999). Flux divergence, indicative of chemical sources/sinks of O_3, on the order of 19% has been reported also by Zeller (1992) over a shortgrass prairie. Without additional gradient measurements of NO and NO_2, these hypothesis, however, cannot be falsified. Excluding these questionable measurements, a paired *t*-Test shows that EC and FG O_3 flux measurements are not statistically different ($p = 0.56$), a finding which holds even when the questionable measurements are included ($p = 0.14$).

With mean maximum daytime O_3 fluxes and deposition velocities of approximately − 8 nmol m^{-2} s^{-1} and 4 mm s^{-1}, our measurements lie in the upper range of literature values reported for grasslands (−4 to −8 nmol m^{-2} s^{-1} and 2–6 mm s^{-1}, respectively; Table 1). Due to the large amount of transpiring plant area (Wohlfahrt and Cernusca, 2002) and the large leaf-level stomatal conductances of the occurring forb and grass species (Wohlfahrt et al., 1998), these relatively high O_3 deposition rates are plausible, even if it has been demonstrated repeatedly that stomatal O_3 deposition may account only for a part of the bulk deposition flux (e.g. Fowler et al., 2001; Meszaros et al., 2009).

4. Summary and conclusions

In this paper we demonstrate the feasibility of making defensible O_3 flux measurements by means of the EC method using a slow-response closed-path scalar sensor. The various sources of flux loss occurring with this approach were corrected for by a series of transfer functions which were used to "degrade" a site-specific reference cospectrum – the ratio between the reference and modified cospectrum was then used to correct fluxes. In contrast to previous studies, we also accounted for the total phase shift, caused by the longitudinal displacement between sonic anemometer and closed-path O_3 analyser, in this fashion by applying a transfer function proposed by Massman (2000). A cospectral analysis confirmed our approach – attenuated reference cospectra compared very well with measured ones. Further justification for the applicability of this approach was derived from a comparison against flux-gradient O_3 flux measurements and a literature review of grassland O_3 fluxes and deposition velocities. The trade-off of our approach were typical daytime correction factors up to 3.5 (i.e. only ca. 28% of the true flux was actually measured) and random uncertainties on the order of 60%.

While it is clearly desirable to measure as much as possible of the true flux and to rely as little as possible on empirical corrections, this paper shows that our understanding of the causes and consequences of various sources of flux loss has sufficiently matured (Shimizu, 2007) so that also less-than-ideal instrumentation may be used in EC flux applications. This paper may thus help to prepare the ground for EC flux measurements of trace gases for which currently no fast-response analysers are available or too costly. Due to the relatively large half-hourly random flux uncertainty, the strength of the proposed approach thereby lies in providing robust average fluxes on longer time scales (i.e. seasonal to inter-annual).

Acknowledgements

This study was financially supported by the Austrian National Science Fund under contract P19849 and the Tyrolean Science Fund under contract Uni-404/486. Family Hofer (Neustift, Austria) is thanked for granting us access to the study site.

References

Asanuma, J., Ishikawa, H., Tamagawa, I., Ma, Y., Hayashi, T., Qi, Y., Wang, J., 2005. Application of the band-pass covariance technique to portable flux measurements over the Tibetan plateau. Water Resources Research 41. doi:10.1029/2005WR003954.

Aubinet, M., Grelle, A., Ibrom, A., Rannik, Ü., Moncrieff, J., Foken, T., Kowalski, A.S., Martin, P.H., Berbigier, P., Bernhofer, Ch., Clement, R., Elbers, J., Granier, A., Grünwald, T., Morgenstern, K., Pilegaard, K., Rebmann, C., Snijders, W., Valentini, R., Vesala, T., 2000. Estimates of the annual net carbon and water exchange of forest: the EUROFLUX methodology. Advances of Ecological Research 30, 113–175.

Baldocchi, D.D., Hicks, B.B., Meyers, T.P., 1988. Measuring biosphere-atmosphere exchanges of biologically related gases with micrometeorological methods. Ecology 69, 1331–1340.

Bassin, S., Calanca, P., Weidinger, T., Gerosa, G., Fuhrer, J., 2004. Modelling seasonal ozone fluxes to grassland and wheat: model improvement, testing and application. Atmospheric Environment 38, 2349–2359.

Cieslik, S., 1998. Energy and ozone fluxes in the atmospheric surface layer observed in southern Germany highlands. Atmospheric Enviroment 32, 1273–1281.

Cieslik, S., 2004. Ozone uptake by various surface types: a comparison between dose and exposure. Atmospheric Environment 38, 2409–2420.

Coyle, M., Nemitz, E., Storeton-West, R., Fowler, D., Cape, J.N., 2009. Measurement of ozone deposition to a potato canopy. Agricultural and Forest Meteorology 149, 655–666.

Davison, B., Brunner, A., Ammann, C., Spirig, C., Jocher, M., Neftel, A., 2008. Cut-induced VOC emissions from agricultural grassland. Plant Biology 10, 76–85.

Finkelstein, P.L., Sims, P.F., 2001. Sampling error in eddy correlation flux measurements. Journal of Geophysical Research 106 (D4), 3503–3509.

Foken, T., Wichura, B., 1996. Tools for quality assessment of surface-based flux measurements. Agricultural and Forest Meteorology 78, 83–105.

Fowler, D., Flechard, C., Cape, J.N., Storeton-West, R.L., Coyle, M., 2001. Measurements of ozone deposition to vegetation quantifying the flux, the stomatal and non-stomatal components. Water, Air and Soil Pollution 130, 63–74.

Grelle, A., 1997. Long-term water and carbon dioxide fluxes from a boreal forest. PhD thesis, Swedish University of Agricultural Sciences.

Grelle, A., Lindroth, A., 1996. Eddy-correlation system for long-term monitoring of fluxes of heat, water vapour and CO_2. Global Change Biology 2, 297–307.

Grünhage, L., Haenel, H.-D., Jäger, H.-J., 2000. The exchange of ozone between vegetation and atmosphere: micrometeorological measurement techniques and models. Environmental Pollution 109, 373–392.

Güsten, H., Heinrich, G., Schmidt, R.W., Schurath, U., 1992. A novel ozone sensor for direct eddy flux measurements. Journal of Atmospheric Chemistry 14, 73–84.

Hammerle, A., Haslwanter, A., Tappeiner, U., Cernusca, A., Wohlfahrt, G., 2008. Leaf area controls on energy partitioning of a temperate mountain grassland. Biogeosciences 5, 421–431.

Haslwanter, A., Hammerle, A., Wohlfahrt, G., 2009. Open- vs. closed-path eddy covariance measurements of the net ecosystem carbon dioxide and water vapour exchange: a long-term perspective. Agricultural and Forest Meteorology 149, 291–302.

Hollinger, D.Y., Richardson, A.D., 2005. Uncertainty in eddy covariance measurements and its application to physiological models. Tree Physiology 25, 873–885.

Horst, T.W., Oncley, S.P., 1995. Flux-PAM measurement of scalar fluxes using cospectral similarity. In: 9th Symposium on Meteorological Observations and Instrumentation. American Meteorological Society, Charlotte, NC/USA.

Horvath, L., Nagy, Z., Weidinger, T., 1998. Estimation of dry deposition velocities of nitric oxide, sulphur dioxide, and ozone by the gradient method above short vegetation during the TRACT campaign. Atmospheric Environment 32, 1317–1322.

Hsieh, C.I., Katul, G., Chi, T.W., 2000. An approximate analytical model for footprint estimation of scalar fluxes in thermally stratified atmospheric flows. Advances in Water Resources 23, 765–772.

Ibrom, A., Dellwik, E., Larsen, S.E., Pilegaard, K., 2007a. On the use of the Webb–Pearman–Leuning theory for closed-path eddy correlation measurements. Tellus 59, 937–946.

Ibrom, A., Dellwik, E., Flyvbjerg, H., Jensen, N.O., Pilegaard, K., 2007b. Strong low-pass filtering effects on water vapour flux measurements with closed-path eddy correlation systems. Agricultural and Forest Meteorology 147, 140–156.

Kaimal, J.C., Finnigan, J.J., 1994. Atmospheric Boundary Layer Flows. Oxford Univ. Press, Oxford, 289 pp.

Massman, W.J., 1991. The attenuation of concentration fluctuations in turbulent flow through a tube. Journal of Geophysical Research 96 (D8), 15259–15268.

Massman, W.J., 2000. A simple method for estimating frequency response corrections for eddy covariance systems. Agricultural and Forest Meteorology 104, 185–198.

Massman, W.J., Lee, X., 2002. Eddy covariance flux corrections and uncertainties in long-term studies of carbon and energy exchange. Agricultural and Forest Meteorology 113, 121–144.

Massman, W.J., MacPherson, J.I., Delany, A., Den Hartog, G., Neumann, H.H., Oncley, S.P., Pearson Jr., R., Pederson, J., Shaw, R.H., 1995. Surface condutances for ozone uptake derived from aircraft eddy correlation data. Atmospheric Environment 29, 3181–3188.

Mauder, M., Foken, T., Clement, R., Elbers, J.A., Eugster, W., Grünwald, T., Heusinkveld, B., Kolle, O., 2008. Quality control of CarboEurope flux data – part 2: inter-comparison of eddy covariance software. Biogeosciences 5, 451–462.

McMillen, R.T., 1988. An eddy correlation system with extended applicability to non-simple terrain. Boundary-Layer Meteorology 43, 231–245.

Meszaros, R., Horvath, L., Weidinger, T., Neftel, A., Nemitz, E., Dämmgen, U., Cellier, P., Loubet, B., 2009. Measurement and modelling ozone fluxes over a cut and fertilized grassland. Biogeosciences Discussions 6, 1069–1089.

Meyers, T.P., Baldocchi, D.D., 2005. Current micrometeorological flux methodologies with application in agriculture. In: Hatfield, J.L., Baker, J.M., Viney, M.K. (Eds.), Micrometeorology in Agricultural Systems. Agronomy Series, 47, pp. 381–396. Madison.

Meyers, T.P., Hall, M.E., Lindberg, S.E., Kim, K., 1996. Use of the modified bowen-ratio technique to measure fluxes of trace gases. Atmospheric Environment 30, 3321–3329.

Meyers, T.P., Finkelstein, P., Clarke, J., Ellestad, G., Sims, P.F., 1998. A multilayer model for inferring dry deposition using standard meteorological measurements. Journal of Geophysical Research 103 (D17), 22645–22661.

Moncrieff, J.B., Malhi, Y., Leuning, R., 1996. The propagation of errors in long-term measurements of land-atmosphere fluxes of carbon and water. Global Change Biology 2, 231–240.

Moncrieff, J.B., Massheder, J.M., de Bruin, H., Elbers, J., Friborg, T., Heusinkveld, B., Kabat, P., Scott, S., Soegaard, H., Verhoef, A., 1997. A system to measure surface fluxes of energy, momentum and carbon dioxide. Journal of Hydrology 188–189, 589–611.

Moore, C.J., 1986. Frequency response corrections for eddy correlation systems. Boundary-Layer Meteorology 37, 17–35.

Ray, D., Stedman, D.H., Wendel, G.J., 1986. Fast chemoluminescent method for measurement of ambient ozone. Analytical Chemistry 58, 598–600.

Richardson, A.D., Hollinger, D.Y., 2005. Statistical modeling of ecosystem respiration using eddy covariance data: maximum likelihood parameter estimation, and Monte Carlo simulation of model and parameter uncertainty, applied to three simple models. Agricultural and Forest Meteorology 131, 191–208.

Rinne, H.J.I., Guenther, A.B., Warneke, C., de Gouw, J.A., Luxembourg, S.L., 2001. Disjunct eddy covariance technique for trace gas flux measurements. Geophysical Research Letters 28 (No. 16), 3139–3142.

Shimizu, T., 2007. Practical applicability of high frequency correction theories to CO_2 flux measured by a closed-path system. Boundary-Layer Meteorology 122, 417–438.

Sillman, S., 1999. The relation between ozone, NO_x and hydrocarbons in urban and polluted rural environments. Atmospheric Environment 33, 1821–1845.

Sorimachi, A., Sakamoto, K., Ishihara, H., Fukuyama, T., Utiyama, M., Liu, H., Wang, W., Tang, D., Dong, X., Quan, H., 2003. Measurements of sulfur dioxide and ozone dry deposition over short vegetation in northern China – a preliminary study. Atmospheric Environment 37, 3157–3166.

Spank, U., Bernhofer, C., 2008. Another simple method of spectral correction to obtain robust eddy-covariance results. Boundary-Layer Meteorology 128, 403–422.

Sun, J., Massman, W., 1999. Ozone transport during the California ozone deposition experiment. Journal of Geophysical Research 104 (D10), 11939–11948.

Swinbank, W.C., 1951. The measurement of vertical transfer of heat and water vapor by eddies in the lower atmosphere. Journal of Atmospheric Science 8, 135–145.

Turnipseed, A.A., Pressley, S.N., Karl, T., Lamb, B., Nemitz, E., Allwine, E., Cooper, W.A., Shertz, S., Guenther, A.B., 2009. The use of disjunct eddy sampling methods for the determination of ecosystem level fluxes of trace gases. Atmospheric Chemistry and Physics 9, 981–994.

Watanabe, T., Yamanoi, K., Yasuda, Y., 2000. Testing of the bandpass eddy covariance method for a long-term measurement of water vapour flux over a forest. Boundary-Layer Meteorology 96, 473–491.

Webb, E.K., Pearman, G.I., Leuning, R., 1980. Correction of flux measurements for density effects due to heat and water vapour transfer. Quarterly Journal of the Royal Meteorological Society 106, 85–100.

Wesely, M.L., Hicks, B.B., 2000. A review of the current status of knowledge on dry deposition. Atmospheric Environment 34, 2261–2282.

Wohlfahrt, G., Cernusca, A., 2002. Momentum transfer by a mountain meadow canopy: a simulation analysis based on Massman's (1997) model. Boundary-Layer Meteorology 103, 391–407.

Wohlfahrt, G., Bahn, M., Horak, I., Tappeiner, U., Cernusca, A., 1998. A nitrogen sensitive model of leaf carbon dioxide and water vapour gas exchange: application to 13 key species from differently managed mountain grassland ecosystems. Ecological Modelling 113, 179–199.

Wohlfahrt, G., Anfang, Ch., Bahn, M., Haslwanter, A., Newesely, Ch., Schmitt, M., Drösler, M., Pfadenhauer, J., Cernusca, A., 2005. Quantifying nighttime ecosystem respiration of a meadow using eddy covariance, chambers and modeling. Agricultural and Forest Meteorology 128, 141–162.

Wohlfahrt, G., Hammerle, A., Haslwanter, A., Bahn, M., Tappeiner, U., Cernusca, A., 2008. Seasonal and inter-annual variability of the net ecosystem CO_2 exchange of a temperate mountain grassland: effects of weather and management. Journal of Geophysical Research 113, D08110. doi:10.1029/2007JD009286.

Yasuda, Y., Watanabe, T., Yamanoi, K., Ohtani, Y., Okano, M., 1997. Measurement of scalar flux from a forest using the bandpass covariance method. Journal of Agricultural Meteorology 42, 493–496.

Zeller, K., 1992. Vertical ozone gradient behaviour and similarity relationship above a flat shortgrass prairie site. In: 10th Symposium on Turbulence and Diffusion of the American Meteorological Society, 29 September–2 October 1992, Portland, OR/USA.

Zeller, K., Hehn, T., 1996. Measurements of upward turbulent ozone fluxes above a subalpine spruce-fir forest. Geophysical Research Letters 23 (8), 841–844.